Research Article

Journal of Labelled Compounds and Radiopharmaceuticals

Received 8 June 2011, Revised 10 August 2011, Accepted 17 August 2011 Published online 23 September 2011 in Wiley Online Library

(wileyonlinelibrary.com) DOI: 10.1002/jlcr.1932

Synthesis of 2-[(4-[^{18}F]Fluorobenzoyloxy) methyl]-1,4-naphthalenedione from 2-hydroxymethyl 1,4-naphthoquinone and 4-[^{18}F]fluorobenzoic acid using dicyclohexyl carbodiimide

Uwe Ackermann,[a,b]* Duanne Sigmund,[a,d] Shinn Dee Yeoh,[a] Angela Rigopoulos,[c] Graeme O'Keefe,[a,b] Glenn Cartwright,[c] Jonathan White,[d] Andrew M. Scott,[a,b,c] and Henri J. Tochon-Danguy[a,b]

2-[(4-[^{18}F]Fluorobenzoyloxy)methyl]-1,4-naphthalenedione ([^{18}F]1) was synthesised as a putative hypoxia imaging agent from 2-hydroxymethyl 1,4-naphthoquinone (7) and 4-[^{18}F]fluorobenzoic acid ([^{18}F]8) using dicyclohexyl carbodiimide (DCC) to activate [^{18}F]8. This coupling reaction was fast and gave quantitative yields. Further investigations are warranted on the use of DCC as a coupling agent in Positron Emission Tomography. The synthesis including HPLC purification and reformulation has been fully automated on a modified FDG synthesiser with two reactor vials. [^{18}F]1 was produced in a radiochemical yield of 27 ± 5%, with a radiochemical purity of 97.5% and a specific activity of 78.4–134.5 GBq/μmol at the end of synthesis (n = 23). The total synthesis time including reformulation was 65 min. [^{18}F]1 was found to be stable in plasma and saline, but underwent rapid metabolism in a phase 1 metabolite assay using rat S9 liver fractions. An *in vivo* evaluation of [^{18}F]1 in transplanted, hypoxic SK-RC-52 tumour-bearing BALB/c nude mice revealed the tumour-to-muscle ratio to be 2.4 ± 0.1 at 2 h post-injection.

Keywords: fluorine-18; PET chemistry; 4-fluorobenzoate; tumor hypoxia; DCC; SK-RC-52 tumors

Introduction

Imaging of hypoxic tissue is of great significance in oncology because hypoxic tumours are more resistant to radiotherapy and chemotherapy than normoxic tumours.[1] For the planning of cancer therapy, the measurement of the hypoxic fraction of tumours is therefore of critical importance.[2,3]

The gold standard for the measurement of oxygen partial pressure (pO_2) is by using a polarographic oxygen electrode.[4] Unfortunately, this is an invasive technique and therefore is not suitable for routine clinical application. Positron Emission Tomography (PET) is noninvasive and offers the potential to measure physiological processes *in vivo*. To date, the most commonly used radiotracers for PET imaging of tumour hypoxia are the nitroimidazole-based compounds [^{18}F]FMISO and [^{18}F]FAZA.[5,6] However, slow accumulation in hypoxic tissue and slow clearance from normoxic tissue result in a low target-to-background ratio and a 2 h delay between tracer administration and actual scanning of the patient. Also, [^{18}F]FMISO only shows uptake in tumours with a pO_2 value below 10 mm Hg, and a differential assessment of tumour hypoxia is therefore not possible. These shortcomings of the existing tracers have sparked the development of new tracers for hypoxia imaging. Most novel tracers reported in the literature have retained the 2-nitroimidazole core as the biologically relevant moiety responsible for the trapping in the hypoxic cell.[7–9] However, in our laboratory we have synthesised two fluorine-18-labelled haloethyl sulfoxides, which we have investigated *in vivo* and *in vitro* as a new class of hypoxia imaging agents.[10]

Although these compounds showed great promise in the imaging of hypoxic tissue in a middle cerebral artery occlusion stroke model in rats, the clinical use of these compounds was deemed unsuitable because their structure is closely related to that of highly toxic nitrogen mustards.

In our search for potential novel hypoxia imaging agents, we have found in the literature that derivatives of 2-hydroxymethyl

[a]*Centre for PET, Austin Health, Melbourne, Australia*

[b]*The University of Melbourne, School of Medicine, Dentistry and Health Sciences, Melbourne, Australia*

[c]*Ludwig Institute for Cancer Research, Melbourne-Austin Branch, Melbourne, Australia*

[d]*The University of Melbourne, Bio21 Institute, Melbourne, Australia*

**Correspondence to: Uwe Ackermann, Centre for PET, Austin Health, Melbourne, Australia.*
E-mail: ackerman@petnm.unimelb.edu.au

Copyright © 2011 John Wiley & Sons, Ltd.

naphthoquinones have the ability to either release cytotoxic compounds under hypoxic conditions or become cytotoxic themselves.[11,12] Figure 1 shows the mechanism by which these quinones can release xenobiotic compounds.

The aim of this project was to couple 2-hydroxymethyl 1, 4-naphthoquinone (**7**) to 4-[^{18}F]fluorobenzoic acid ([^{18}F]**8**), and to investigate the *in vitro* and *in vivo* properties of this putative tracer using hypoxic SK-RC-52 tumours.

Results and discussion

Chemistry

Precursor and F-19 standard synthesis

Figure 2 shows the synthesis of 2-hydroxymethyl 1,4-naphthoquinone (**7**), which was achieved by following the procedures reported in the literature.

Commercially available 1,4-naphthoquinone (**2**) was reacted with $SnCl_2$ and MeOH/HCl to form 1,4-dimethoxynaphthalene (**3**).[13] Bromination of 1,4-dimethoxynaphthalene (**3**) gave 2-bromo 1,4-dimethoxynaphthalene (**4**), which was subsequently converted to 1,4 dimethoxynaphthalene-2-carbaldehyde (**5**) via a Grignard reaction.[14] Reduction of this compound to 2-hydroxymethyl 1,4-dimethoxynaphthalene (**6**) was achieved with sodium borohydride as reducing agent.[15] The desired 2-hydroxymethyl 1,4-naphthoquinone (**7**) was then synthesised from 2-hydroxymethyl 1,4-dimethoxynaphthalene (**6**) by cerium ammonium nitrate oxidation.[15]

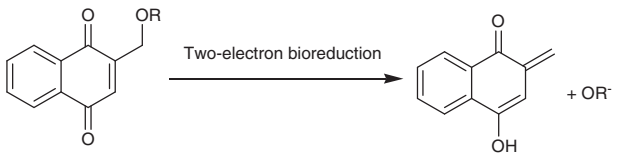

Figure 1. Release of cytotoxic compounds under bioreductive conditions.

The cold standard for tracer identification and measurement of specific activity was synthesised from 4-[^{19}F]fluorobenzoic acid (**8**) and 2-hydroxymethyl 1,4-naphthoquinone (**7**) using dicyclohexyl carbodiimide (DCC) for the esterification step (Figure 3).

The cold standard was characterised by NMR and high-resolution MS. The elution profile of [^{19}F]**1** was determined using an LCMS system for future independent quality control of the radiotracer. The UV active peak at 18.3 min showed a mass spectrum consistent with the structure of **1**. Characteristic ions were $[C_7H_5FO_2 + NaCH_3CN(H_2O)_1]^+$ ($m/z = 222$), $[M\text{-}C_7H_3FO_2 + H(H_2O)_5]^+$ ($m/z = 263$), and $[M + H]^+$ ($m/z = 311$).

Radiolabelling

4-[^{18}F]fluorobenzoic acid was produced from (4-ethoxycarbonylphenyl) trimethylammonium triflate (**9**) via an aromatic nucleophilic substitution mechanism using a dried [^{18}F]KF/Kryptofix complex.[16] After hydrolysis of the intermediate ethyl 4-[^{18}F] fluorobenzoate ([^{18}F]**10**) with tetramethylammonium hydroxide followed by addition of acetic acid, 4-[^{18}F]fluorobenzoic acid ([^{18}F]**8**) was obtained in a radiochemical yield of 34 ± 5%. The compound was trapped on a C-18 SepPak and eluted with acetonitrile into a second reactor vial. [^{18}F]**1** was obtained by reacting quinone **7** with 4-[^{18}F]fluorobenzoic acid ([^{18}F]**8**) in the presence of DCC (Figure 4).

Semi-preparative HPLC separation was carried out using an isocratic 60:40 acetonitrile/0.1 M ammonium formate mobile phase on an Alltech Apollo™ C-18 column at a flow rate of 4 mL/min. The retention time of the tracer was 16 min. After HPLC separation, the radiotracer was reformulated in 10 mL of 10% ethanol/saline.

Independent quality control was performed using a radio-HPLC system. The radioactive and UV active peaks observed were at identical retention times as the cold standard (18.3 min).

Radiochemical yield was 27 ± 5% (2.16 ± 0.4 GBq from 8.1 GBq of [^{18}F]fluoride), radiochemical purity was 97.5%, and specific activity was 78.4–134.5 GBq/μmol at the end of synthesis ($n = 23$).

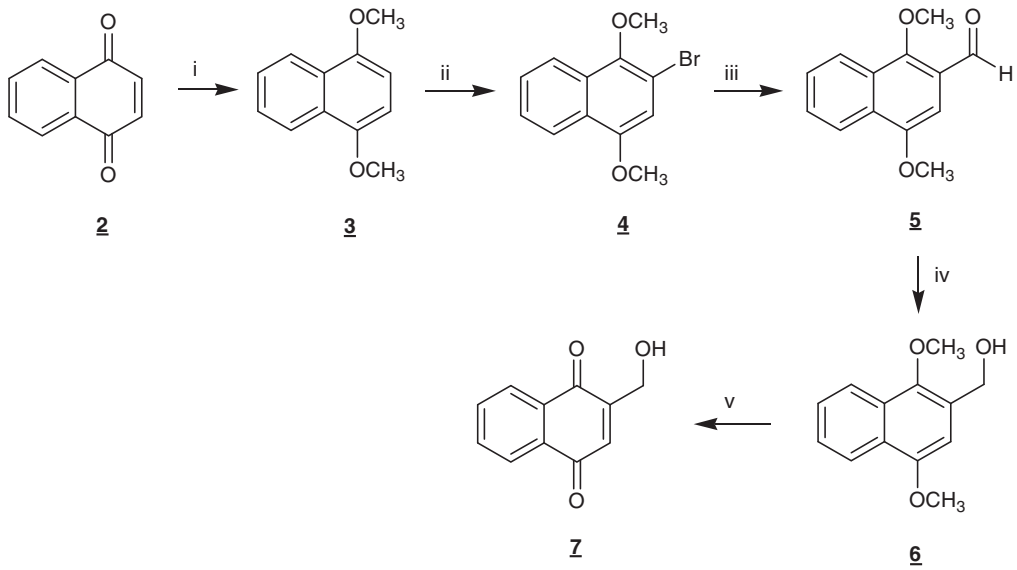

Reagents and conditions: i: HCl, MeOH, $SnCl_2$; ii: Br_2, Fe, $CHCl_3$; iii: Mg, DMF, THF; iv: $NaBH_4$; v: CAN, CH_3CN

Figure 2. Synthesis of 2-hydroxymethyl 1,4-naphthoquinone precursor.

Copyright © 2011 John Wiley & Sons, Ltd.

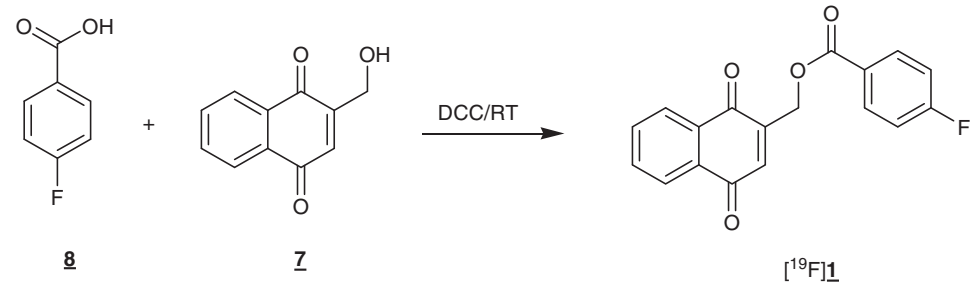

Figure 3. Synthesis of cold standard [^{19}F]**1**.

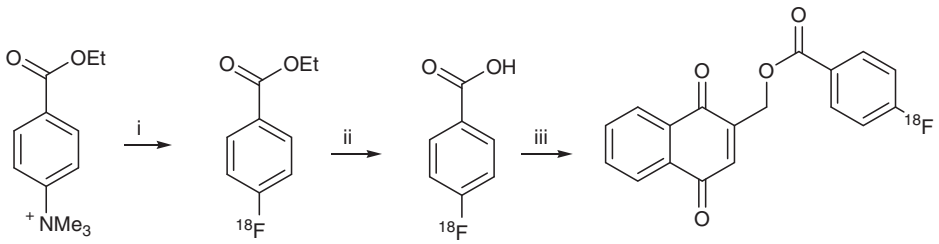

Reagents and conditions: i: [^{18}F]KF/kryptofix, 110°C; ii: NMe_4OH, 90°C; iii: 2-hydroxymethylnaphthoquinone, DCC, 40°C

Figure 4. Synthesis of [^{18}F]**1**.

The radiosynthesis including reformulation was fully automated using a modified FDG synthesiser with two reactor vials.[17] The total synthesis time including reformulation was 65 min.

It is worth noting that the addition of acetic acid after base hydrolysis is crucial to the success of the synthesis. Attempts to produce [^{18}F]**1** by omitting this step were unsuccessful.

To our knowledge, this is also the first time that a DCC-mediated coupling was used for the synthesis of a PET radiotracer. The quantitative yield and short reaction time may make this an interesting method for other applications.

In vitro studies

Lipophilicity

The octanol/water coefficient was measured and the log*P* was calculated to be 2.7, thus indicating that [^{18}F]**1** has a lipophilicity suitable for crossing cell membranes. In the literature, the log*P* values for FAZA and FMISO were calculated using HPLC retention times and were found to be 1.1 and 2.6, respectively.[18] However, when measured using octanol/water distribution, the log*P* for FMISO was found to be −0.33.[19] In our laboratory, with the octanol/water distribution method, the log*P* for FMISO was 0.05.

Stability and metabolite studies

The compound was found to be stable in human plasma, saline, and potassium phosphate buffer (pH 7.4) for a period of more than 2 h.

As a model for radiotracer metabolism *in vivo*, we used a phase 1 metabolism *in vitro* assay using rat S9 liver fractions.[20] Phase 1 metabolism is predominantly catalysed by the cytochrome P450 (CyP450) family of enzymes, which is found on the endoplasmic reticulum, with the active site facing the cytosol.[21] All members of this family have a haeme group, which enables them to bind oxygen and receive electrons from NADPH. Through a controlled radical reaction, this catalytic system has the ability to hydroxylate xenobiotic compounds. When conducted *in vitro*, this assay requires the addition of either NADPH or an NADPH-generating system.[22] In this study, we have decided to use an NADPH-generating system, which consisted of NADP, $MgCl_2 \times 6H_2O$, glucose 6-phosphate, and glucose 6-phosphate dehydrogenase.[23] Since a maximum incubation time of 2 h is generally considered sufficient for fluorine-18-labelled tracers, we used four time points (30, 60, 90, and 120 min) to measure tracer stability.[24] For each time point, 300 μL of a solution of S9 liver fractions, the NADPH-generating system, and the reformulated radiotracer were incubated at 37 °C in an Eppendorf tube. After the required incubation time, the reaction was quenched by the addition of methanol, the sample centrifuged and analysed by metabolite HPLC. Experiments were done in triplicates for statistical reliability.

Our assay revealed that the compound underwent rapid metabolism, with only 14.4% of the tracer intact after 60 min and 3.4% of the tracer still intact at the end of the observation period of 120 min. Figure 5 shows the average per cent of intact tracer over time with error bars. The percentage of unchanged **1** was fitted using Microsoft Excel software. The following single exponential equation:

$$y = 100 \times e^{-0.0304t}$$

where *y* is the percentage of intact tracer was found to describe the radiotracer kinetics with $R^2 = 0.9756$. From this formula, a biological half-life of 22.8 min could be calculated.

At least six polar radioactive metabolites could be detected over the observed period of the assay. Figure 6 shows a representative chromatogram of the S9 liver fraction assay at 60 min post-incubation.

The retention time of [^{18}F]**1** under the conditions of the HPLC conditions was 17.6 min. 4-[^{18}F]Fluorobenzoic acid (**8**), which we

Copyright © 2011 John Wiley & Sons, Ltd.

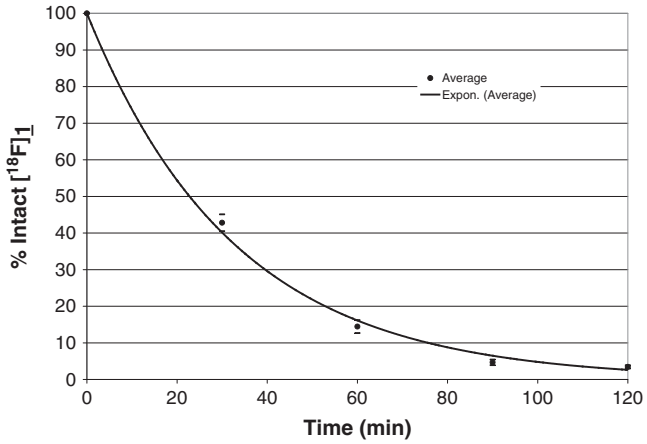

Figure 5. Metabolism of [^{18}F]**1** over time with S9 liver fractions.

expected to be a major metabolite, was observed at 11.9 min. As shown in Figure 7, this metabolite can either be formed by simple hydrolysis of the starting material [^{18}F]**1** or by oxidation of the benzylic function followed by elimination of [^{18}F]**8**.

It is therefore surprising that the radioactive peak corresponding to [^{18}F]**8** represents only 12.5% of the total radioactivity of all metabolites at 60 min post-incubation. The appearance of a polar metabolite at 11.4 min may point to hydroxylation of 4 [^{18}F]fluorobenzoic acid ([^{18}F]**8**), which could occur either before or after cleavage from the 2-[(4-[^{18}F]fluorobenzoyloxy)methyl]-1,4-naphthalenedione ([^{18}F]**1**) parent molecule.

A control incubation with the NADPH-generating system only showed that [^{18}F]**1** was stable towards reduction by NADPH. We have also found that [^{18}F]FMISO does not undergo phase 1 metabolism with our S9 liver fraction assay over a period of 2 h and is also stable towards NADPH reduction.

In vivo experiments

In vivo testing of the compound was carried out using transplanted SK-RC-52 tumours, which were grown in the shoulders of BALB/c nude mice.[25] A static, 10 min frame 2 h after tracer administration was acquired for four mice to measure the tumour-to-muscle ratio. The tumour-to-muscle ratio for the four mice investigated was found to be 2.4 ± 0.1. Figure 8 shows a representative image of the uptake of [^{18}F]**1** in a BALB/c nude mouse bearing a 495 mm^3 SK-RC-52 tumour.

After imaging, the oxygen partial pressure in the centre and periphery of all tumours was measured using an oxygen electrode.[25,26] All tumours were found to have pO_2 levels of below 10 mm Hg in the central region, thus making them a good model for tumour hypoxia. Owing to the heterogeneity of tumours, the pO_2 value measured at the periphery was found to be greater than 10 mm Hg. The small-animal PET images also revealed that the majority of the radioactivity was found in the bowel, and we believe that clearance of [^{18}F]**1** occurs mainly through this organ.

Although tumour hypoxia imaging with [^{18}F]**1** seems feasible, we believe that modifications to the chemical structure of this lead compound are necessary to improve the *in vivo* and *in vitro* properties. Depending on the substituents attached to the 1,4- naphthoquinone core, reduction potentials between -0.16 V and -0.42 V have been reported in the literature.[27] The reported value for [^{18}F]FMISO (-0.389 V) falls well within this range, and 1,4-naphthoquinone-based imaging agents therefore offer the exciting prospect of fine-tuning hypoxia selectivity.[6] The observed tumour-to-muscle ratio of [^{18}F]**1** (2.4 ± 0.1) is lower than the literature reported value for [^{18}F]FMISO uptake (4.4 ± 1) in mice bearing a C3H mammary carcinoma.[28] Potentially, this may be improved if irreversible trapping of the imaging agent in hypoxic tissue can be achieved.

Experimental

General

No-carrier-added [^{18}F]fluoride was produced by the ^{18}O(p,n)^{18}F nuclear reaction with a 10 MeV proton beam generated by the IBA Cyclone 10/5 cyclotron in a titanium target using [^{18}O]H_2O at Austin Health, Centre for PET. Typical irradiation parameters were 20 μA for 30 min, which resulted in 5.4–8.1 GBq (146–219 mCi) of [^{18}F]fluoride being transferred into the synthesis module. These yields represent around 25% of the theoretical yield and are explained by the use of recycled [^{18}O]H_2O of unknown isotopic enrichment. Isolation of the [^{18}F]fluoride ion from [^{18}O]H_2O was achieved by trapping on a QMA ion exchange column. Elution of the column with a solution containing anhydrous K_2CO_3

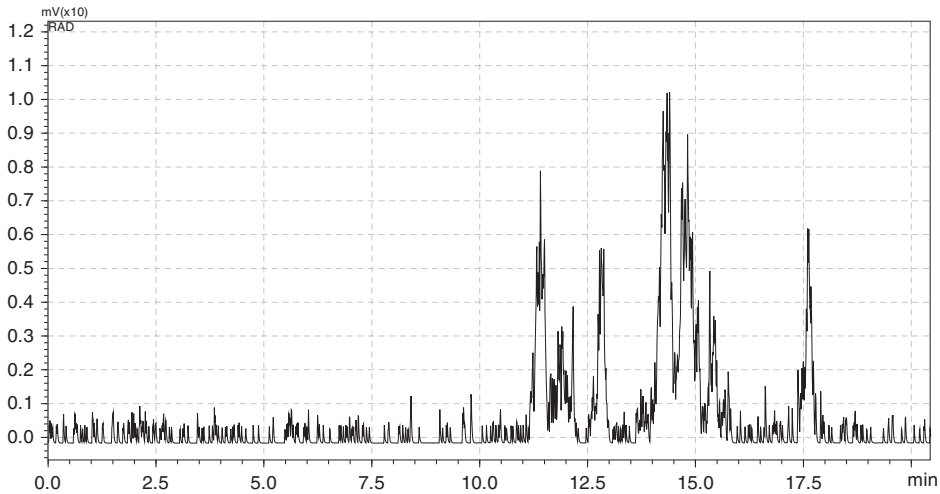

Figure 6. Representative HPLC chromatogram of [^{18}F]**1** metabolite assay after 60 min.

Copyright © 2011 John Wiley & Sons, Ltd.

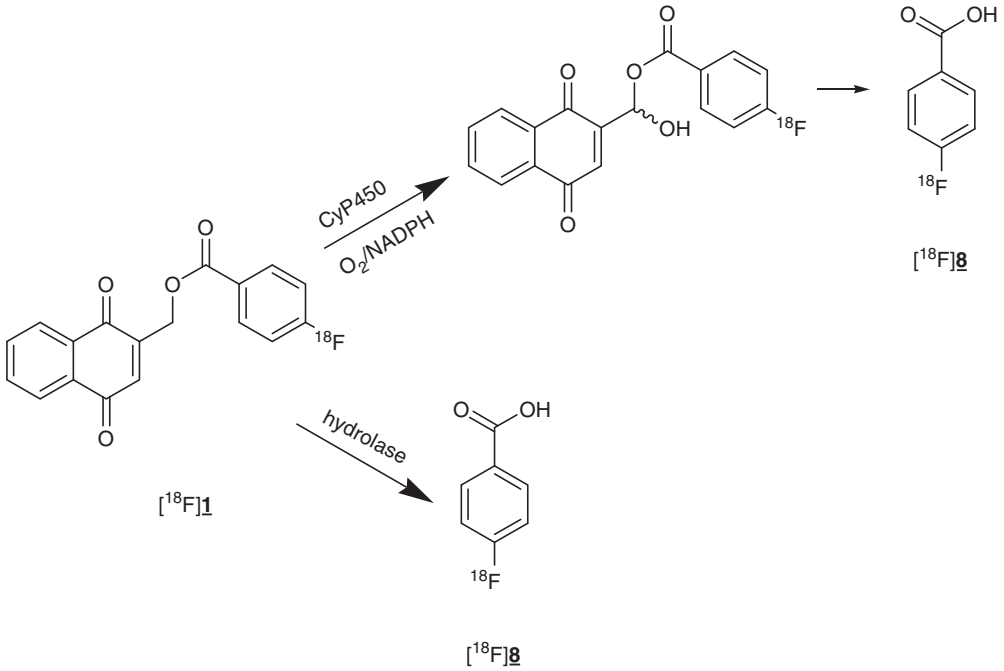

Figure 7. Potential metabolic pathways for the formation of [^{18}F]**8**.

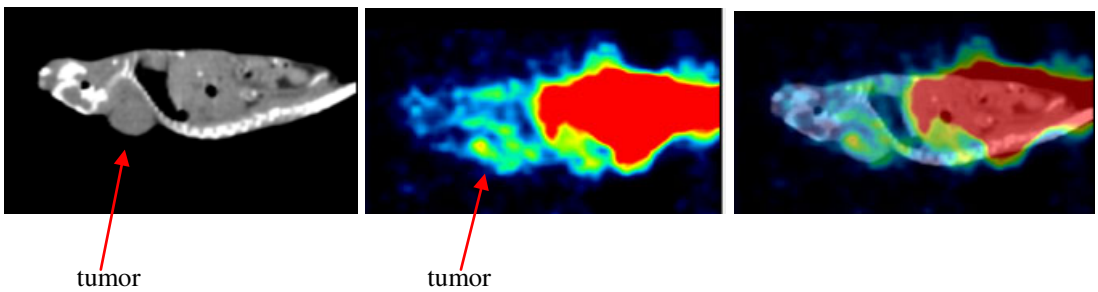

Figure 8. CT (left) and PET (centre) co-registered (right) sagittal view of [^{18}F]**1** uptake in an SK-RC-52 tumour-bearing mouse.

(0.025 mmol) and 20 mg of Kryptofix 2.2.2 (0.053 mmol) in 0.4 mL of acetonitrile plus 0.2 mL of water followed by repeated (3 times, 1.5 mL each) azeotropic evaporation with acetonitrile to dryness gave the anhydrous [^{18}F]fluoride complex used in the labelling experiments.

Solvents were purchased from Merck and used as received. Reagents were purchased from Sigma-Aldrich and used without further purification. Flash chromatography was performed on a Grace Davison Reveleris™ Flash Chromatography System using Reveleris™ Flash Cartridges.

Semi-preparative HPLC was performed using a Shimadzu LC-10AS isocratic pump equipped with a 5 mL injection loop and a reversed phase column (Alltech Apollo™ C-18, 5 μm, 10 × 250 mm). An isocratic mobile phase of 60:40 acetonitrile/0.1 M ammonium formate was used as eluent at a flow rate of 4 mL/min. Detection of chemical compounds was achieved with a Shimadzu SPD-6AV UV detector (254 nm) and a Geiger-Müller tube as radiodetector.

For LCMS measurements, a Shimadzu 2010 LCMS system equipped with a 5 μL injection loop, an SPD-20A UV-Vis detector, and two LC-20AD solvent pumps for high-pressure mixing of mobile phases were used. The stationary phase was a Phenomenex Gemini C-18 reversed phase column (10 μm, 150 × 4.6 mm). Acetonitrile (A) and water (B) with 0.1% formic acid were used as the mobile phase, and a gradient elution technique was used for the analysis: 0–18 min: 45–90% A, 18–30 min: isocratic 90% A at a flow rate of 0.5 mL/min. The same system was used for independent quality control. However, the MS was replaced with an in-house built flow-through detector with a Geiger-Müller tube for the detection of radioactive compounds.

For radiotracer stability studies, a Shimadzu HPLC system equipped with a 20 μL injection loop, a SPD-20A UV-Vis detector, and two LC-20AD solvent pumps for high-pressure mixing of mobile phases were used. The stationary phase was a Grace Davison Vision reversed phase column (5 μm, 150 × 4.6 mm). Acetonitrile (A) with 0.1% formic acid and water (B) with 0.1% formic acid were used as the mobile phase, and a gradient elution technique was used for the analysis: 0–18 min: 5–90% A, 18–30 min: isocratic 90% A at a flow rate of 0.5 mL/min. For the detection of radioactive compounds, a Bioscan dual BGO coincidence detector was used. A CAT Thermo Shaker SH26.3 was used to incubate the radiotracer with rat S9 liver fractions and the NADPH-generating system. Statistical calculations were performed using Microsoft Excel 2003.

^{1}H and ^{13}C NMR spectra were recorded on a Varian Unity 500 NMR spectrometer operating at 500 and 125 MHz, respectively.

Copyright © 2011 John Wiley & Sons, Ltd.

Chemistry

Cold chemistry

2-[(4-Fluorobenzoyloxy)methyl]-1,4-naphthalenedione. 4-Fluorobenzoic acid (**8**) (140 mg, 1 mmol) and DCC (247 mg, 1.2 mmol) were dissolved in 5 mL of dry DMSO, and the solution was stirred at room temperature for 5 min. 2-Hydroxy 1,4-naphthoquinone (**7**) (188 mg, 1 mmol) in 3 mL of dry acetonitrile was added, and the reaction mixture was stirred for 24 h. Then, 10 mL of water was added, and the mixture was purified using the Reveleris™ system with a 12 g Reveleris reversed phase C-18 column as stationary phase and an acetonitrile (A)/water (B) gradient system as mobile phase. The gradient system used was 0–3 min: 45% A, 3–19.8 min: 74% A, 19.8–22.5 min: 100% A, and 22.5–30 min: 100% A. The peak at 14.8 min was collected, and the solvent evaporated to give 264 mg (85%) of pure **1**.

^{1}H NMR ($CDCl_3$) δ: 5.41 (s, 2H), 6.99 (s, 1H), 7.158–7.236 (m, 4H), 7.78–7.89 (m, 2H), 8.103–8.121 (m, 2H).

^{13}C NMR ($CDCl_3$) δ: 60.50, 115.75, 115.92, 125.51, 126.41, 126.52, 131.93, 132.38, 132.46, 133.66, 133.99, 134.19, 145.21, 164.72, 165.12, 167.15, 184.04, 184.48.

HRMS ($C_{18}H_{11}FO_4$) (M + Na) measured (*m/z*): 333.05319, calcd.: 333.05391.

Radiochemistry

*4-[^{18}F]Fluorobenzoic acid ([^{18}F]**8**).* (4-Ethoxycarbonylphenyl) trimethylammonium triflate (**9**) (5 mg, 20 μmol) in 1 mL of DMSO was added to the dried [^{18}F]KF/Kryptofix complex, and the mixture was heated to 110 °C for 15 min. Twenty microlitres of an aqueous 1 M solution of tetramethylammonium hydroxide (20 μmol) in 1 mL of acetonitrile was then added. The mixture was heated to 110 °C for 15 min in an open vial to evaporate excess water through azeotropic distillation with acetonitrile and hydrolyse the intermediate ethyl 4-[^{18}F]fluoro benzoate ([^{18}F]**10**). Then, 3 mL of 6% acetic acid and 6 mL of water were added, and 4-[^{18}F]fluorobenzoic acid ([^{18}F]**8**) was loaded on a C18 SepPak cartridge. After washing with 5 mL of water and drying of the C-18 SepPak cartridge, 4-[^{18}F]fluorobenzoic acid ([^{18}F]**8**) was eluted with 1 mL of acetonitrile into a second reactor vial.

*2-[(4-[^{18}F]Fluorobenzoyloxy)methyl]-1,4-naphthalenedione ([^{18}F]**1**).* To the second reactor vial was then added a mixture 2 mg of 2 hydroxymethyl 1,4-naphthoquinone (**7**) (0.01 mmol) and 20 mg of DCC (0.097 mmol) in 1 mL of acetonitrile. After heating to 40 °C for 10 min, 3 mL of aqueous 0.1 M ammonium formate was added, and the reaction mixture was purified using the semi-preparative HPLC system as described above. The retention time of [^{18}F]**1** was 16 min. Reformulation in 10% ethanol gave 2-(1,4-naphthoquinonyl)methyl 4-[^{18}F]fluorobenzoate ([^{18}F]**1**) in 27 ± 5% radiochemical yield with a specific radioactivity of 78.4–134.5 GBq/μmol and a radiochemical purity of 97.5%. Independent quality control was carried out using a radio-HPLC system.

In vitro studies

Stability in saline and plasma

The *in vitro* stability of [^{18}F]**1** was assessed by incubating 1 mCi of radioactivity at 37 °C in 2 mL of saline or plasma over a period of 2 h. Two millilitres of acetonitrile was added to the plasma sample to precipitate the proteins. The sample was spun down, and the supernatant analysed by metabolite HPLC. No radioactive metabolites could be detected.

Metabolite studies using rat S9 liver fractions

Preparation of the NADPH-generating system. In 4 mL of 100 mM potassium phosphate (pH 7.4) were dissolved 37.2 mg (0.132 mmol) of glucose 6-phosphate, 39.8 mg (0.052 mmol) of NADP, and 11.5 U of glucose 6-phosphate dehydrogenase. A solution of 26.8 mg (0.132 mmol) of $MgCl_2 \times 6H_2O$ in 1 mL of water was added to the mixture, and the mixture was stored on ice.

S9 liver fraction assay. For each of the four time points (30, 60, 90, and 120 min), 15 μL of rat S9 liver fractions (20 mg/mL), 40 μL of the NADPH-generating system, 15 μL of the reformulated radiotracer, and 230 μL of 100 mM potassium phosphate buffer (pH 7.4) (total volume 300 μL) were combined in an Eppendorf tube and incubated at 37 °C using a thermo shaker. After the required incubation time, the reaction was quenched by adding 150 μL of methanol. The sample was then centrifuged for 10 min at 11 000 rcf, and 20 μL of the supernatant was injected into the metabolite HPLC.

LogP measurement. Log*P* was measured by mixing 8 MBq (typically around 40 μL of the final formulation) of the tracer with 1 g each of 1-octanol and phosphate buffer (0.1 M, pH 7.4) in a test tube. The test tube was vortexed for 3 min at room temperature, followed by centrifugation for 5 min at 9300 rcf. Two weighed samples (0.5 g each) from the 1-octanol and buffer layers were then measured for radioactivity using a Wallac Wizard well counter. The partition coefficient was calculated from the ratio of cpm/g of 1-octanol to that of buffer.

In vivo animal experiments

All animal experiments were approved by the Austin Health animal ethics committee.

Generation of tumour transplants

SK-RC-52 tumours were first grown by subcutaneously injecting suspensions of 6×10^6 SK-RC-52 cells into the flank of BALB/c nude mice. Tumours were allowed to grow to a size of 300 mm^3, transplanted into the shoulder of BALB/c nude mice, and allowed to grow to a size of ~500 mm^3 for imaging studies.

Small animal imaging

Imaging studies were performed using a Philips Mosaic small-animal PET scanner. Animals were injected with 12.95 MBq of radiotracer in 100 μL of the final formulation and anaesthetized using isoflurane delivered by the Minerva Biovet animal imaging system before scanning. The Minerva Biovet system also provides a temperature-stabilised environment for the animals during the induction and imaging stages. Two hours after injection, a 10-min static frame was acquired and images were reconstructed using the RAMLA3D algorithm.[29] Following PET image acquisition, the animals were relocated to a Philips Gemini PET/CT and CT scanned at 90 kVp with a 150-mA tube current at 0.5 s per rotation. The acquired CT had a pixel size of 0.098 mm and a slice thickness of 0.6 mm. The resultant PET and CT images were then imported into the PMOD analysis system for spatial alignment and subsequent volume-of-interest analysis.

Copyright © 2011 John Wiley & Sons, Ltd.

Polarographic pO_2 measurements

After imaging, animals were humanely euthanized, and the oxygen partial pressure in the tumour was measured using a polarographic oxygen electrode.[26] Tumour pO_2 was measured with a two-channel time-resolved luminescence-based optical oxygen-sensing probe (Oxylite 2000, Oxford Optronix, Oxford, UK) or Oxylite probe. The probes (230 μm o.d.) were precalibrated by the manufacturer (±0.7 mmHg or <±10% of actual pO_2, whichever was greater). To further ensure correct pO_2 readings in the experiments, the probe was checked in normal saline and again in animals just killed to ensure a 0 mm Hg recording.

Conclusion

2-(1,4-Naphthoquinonyl)methyl 4-[^{18}F]fluorobenzoate ([^{18}F]**1**) has been synthesised as a putative hypoxia tracer from 2-hydroxymethyl 1,4-naphthoquinone (**7**) and 4-[^{18}F]fluorobenzoic acid ([^{18}F]**8**) using DCC to activate [^{18}F]**8**. The synthesis has been automated using a modified FDG synthesiser. [^{18}F]**1** has been produced in a radiochemical yield of 27 ± 5%, with a radiochemical purity of 97.5% and a specific activity of 78.4–134.5 GBq/μmol at the end of synthesis.

The results of our *in vivo* evaluation indicate that imaging of tumour hypoxia with radiolabelled quinones is feasible. However, improvements to the overall structure of [^{18}F]**1** are required to make this molecule more stable towards liver metabolism and achieve irreversible trapping in hypoxic cells. The formation of [^{18}F]**1** from the intermediate acid [^{18}F]**8** using DCC was fast and quantitative. We therefore believe that the use of DCC as a coupling reagent in PET deserves further investigation.

Acknowledgements

This work was supported by a grant from the National Health and Medical Research Council project (grant no. 469002) and a grant from the Perpetual Trustees H&L Hecht Trust.

References

[1] J. Overgaard, J. R. Horsmann, *Sem Radiat Oncol.* **1969**, *6*, 10–21.
[2] J. G. Rajendran, K. R. G. Hendrickson, A. M. Spence, M. Muzi, K. A. Krohn, D. A. Mankoff, *Eur. J. Nucl. Med. Mol. Imaging.* **2006**, *33*, S44-S53.
[3] D. M. Brizel, R. K. Dodge, R. W. Clough, M. W. Dewhirst, *Radiother. Oncol.* **1999**, *53*, 113–117
[4] B. Gagel, P. Reinartz, E. DiMartino, M. Zimny, M. Pinkawa, P. Maneschi, S. Stanzel, K. Hamacher, H. H. Coenen, M. Westhofen, U. Buell, M. J. Eble, *Q. J. Nucl. Med.* **2001**, *45*, 138–188.
[5] H. J. Tochon-Danguy, J. I. Sachinidis, F. Chan, J.G. Chan, C. Hall, L. Cher, S. Stylli, J. Hill, A. Kaye, A. M. Scott, *Nucl. Med. Biol.* **2002**, *29*, 191–197.
[6] M. Piert, H.-J. Machulla, M. Picchio, G. Reischl, S. Ziegler, P. Kumar, H.-J. Wester, R. Beck, A. J. B. McEwan, L. I. Wiebe, M. Schwaiger, *J. Nucl. Med.* **2005**, *46*, 106–113.
[7] L. Dubois, W. Landuyt, L. Cloetens, A. Bol, G. Bormans, K. Haustermans, D. Labar, J. Nuyts, V. Grégoire, L. Mortelmans, *Eur. J. Nucl. Med. Mol. Imaging* **2009**, *36*, 209–218.
[8] J. van Loon, M. H. M. Janssen, M. Öllers, H. J. W. L. Aerts, L. Dubois, M. Hochstenbag, A.-M. C. Dingemans, R. Lalisang, B. Brans, B. Windhorst, G. A. van Dongen, H. Kolb, J. Zhang, D. De Ruysscher, P. Lambin, *Eur. J. Nucl. Med. Mol. Imaging* **2010**, *37*, 1663–1668.
[9] C. J. Koch, J. S. Scheuermann, C. Divgi, K. D. Judy, A. V. Kachur, R. Freifelder, J. S. Reddin, J. Karp, J. B. Stubbs, S. M. Hahn, J. Driesbaugh, D. Smith, S. Prendergast, S. M. Evans, *Eur. J. Nucl. Med. Mol. Imaging* **2010**, *37*, 2048–2059.
[10] C. L. Falzon, U. Ackermann, N. Spratt, H. J. Tochon-Danguy, J. White, D. Howells, A. M. Scott, *J Labelled Cpd Radiopharm* **2006**, *49*, 1089–1103.
[11] I. Antonini, T.-S. Lin, L. A. Cosby, Y.-R. Dai, A. C. Sartorelli, *J. Med. Chem.* **1982**, *25*, 730–735.
[12] C. Flader, J. Liu, R. F. Borch, *J. Med. Chem.* **2000**, *43*, 3157–3167.
[13] K. Karichiappan, D. Wege, *Aust. J. Chem.* **2000**, *53*, 743–747.
[14] H. Uno, *J. Org. Chem.* **1986**, *51*, 350–358.
[15] K. Kobayashi, M. Ushida, T. Uneda, K. Yoneda, M. Tanmatsu, O. Morikawa, H. Konishi, *J. Chem. Soc. Perkin. Trans. 1.* **2001**, 2977–2982.
[16] G. Tang, W. Zeng, M. Yu, G. Kabalka, *J. Labelled Compd. Radiopharm.* **2008**, *51*, 68–71.
[17] S. D. Yeoh, U. Ackermann, H. J. Tochon-Danguy, J. Sachinidis, R. Mulligan, S. Poniger, *J. Label. Compd Radiopharm.* **2009**, *52*, Supplement 1 S289
[18] P. Kumar, D. Stypinski, H. Xia, A. J. B. McEwan, H.-J. Machulla, L. I. Wiebe, *J. Labelled. Compds. Radiopharm.* **1999**, *42*, 3–16.
[19] R. Bejot, V. Kersemans, C. Kelly, L. Carroll, R. C. King, V. Gouverneur, *Nucl. Med. Biol.* **2010**, *37*, 565–575.
[20] S. Yoshihara, M. Makishima, N. Suzuki, S. Ohta, *Toxicol. Sci.*, **2001**, *62*, 221–227.
[21] C. J. Patten, *Drug Discov. Today: Technol.* **2006**, 73–78.
[22] N. Plant, *Drug Discov. Today*. **2004**, *9*, 328–336.
[23] D. C. Ackley, K. T. Rockich, T. R. Baker, *Methods in Pharmacology and Toxicology: Optimization in Drug Discovery: In Vitro Methods*, 1st Edition **2004**, 151–162, ISBN: 978-1-61737-499-9, Springer, Humana Press.
[24] T. L. Ross, M. Honer, P. Y. H. Lam, T. L. Mindt, V. Groehn, R. Schibli, P. A. Schubiger, S. M. Ametamey, *Bioconjugate Chem.* **2008**, *19*, 2462–2470.
[25] N. Lawrentschuk, A. M. Poon, S. S. Foo, L. G. Putra, C. Murone, I. D. Davis, D. M. Bolton, A. M. Scott, *BJU Int.* **2005**, *96*, 540–6.
[26] N. Lawrentschuk, F. T. Lee, G. Jones, A. Rigopoulos, A. Mountain, G. O'Keefe, A. T. Papenfuss, D. M. Bolton, I. D. Davis, A. M. Scott, *Urol. Oncol.* **2009**, Jun 12. doi:10.1016/j.urolonc.2009.03.028 [Epub ahead of print]
[27] J. Koyama, I. Morita, N. Kobayashi, T. Osakai, H. Hotta, J. Takayasu, H. Nishino, H. Tokuda, *Cancer Lett.* **2003**, *201*, 25–30.
[28] T. Grönroos, L. Bentzen, P. Marjamäki, R. Murata, M. R. Horsman, S. Keiding, O. Eskola, M. Haaparanta, H. Minn, O. Solin, *Eur. J. Nucl. Med. Mol. Imaging*. **2004**, *31*, 513–520.
[29] J. Browne, A. B. de Pierro, *IEEE Trans. Med. Imaging*, **1996**, *15*, 687–699.

Copyright © 2011 John Wiley & Sons, Ltd.